ELSEVIER

Journal of Alloys and Compounds 265 (1998) 70–76

Journal of ALLOYS AND COMPOUNDS

Mössbauer spectral and magnetic investigations of $RFe_{10}Cr_2$ compounds (R=rare earth)

J.J. Bara[a,*], B.F. Bogacz[a], A.T. Pędziwiatr[a], P. Stefański[b], A. Szlaferek[b], A. Wrzeciono[b]

[a]*Institute of Physics, Jagiellonian University, Reymonta 4, 30-059 Cracow, Poland*
[b]*Institute of Molecular Physics, Polish Academy of Science, Smoluchowskiego 17/19, 60-179 Poznań, Poland*

Received 4 July 1997

Abstract

The results of X-ray diffraction, magnetic susceptibility and Mössbauer investigations of $RFe_{10}Cr_2$ intermetallic compounds (R=Y, Nd, Gd, Tb, Dy, Ho, Er and Tm) are presented and discussed. The variation with a sample composition of the lattice constants, unit cell volume, Curie temperature, iron and rare earth magnetic moments, magnetic anisotropy field and ^{57}Fe hyperfine interaction parameters are shown. The Curie temperatures of the $RFe_{10}Cr_2$ series follow the same trend as in other R-Fe compounds and range from 466 K (for $TmFe_{10}Cr_2$) to 585 K (for $GdFe_{10}Cr_2$). Spin reorientation transition phenomena caused by the competition between the rare earth and iron sublattice magnetic anisotropies are observed for R=Tb, Dy and Er. The sample composition has little influence on the ^{57}Fe hyperfine interaction parameters. The numerical analysis of Mössbauer spectra shows that chromium atoms have a pronounced preference for occupying 8i sublattice in the whole series of the investigated compounds. From the magnetic susceptibility and Mössbauer data the approximate values of iron and rare earth magnetic moments are derived.

Keywords: Mössbauer effect; Intermetallic compounds; Magnetic properties of $RFe_{10}Cr_2$

1. Introduction

The properties of ternary rare earth iron-rich compounds of the type $RFe_{12-x}M_x$ (R=Y, Nd, Sm, Gd, Tb, Dy, Ho, Er, Tm and Lu, with M=Si, Ti, V, Cr, Mo and W) have been studied intensively [1–11] and were reviewed [12,13]. Those studies have been stimulated for a great deal by the possibility of using some of these materials for high performance permanent magnet applications. The $RFe_{12-x}M_x$ compounds are based on the tetragonal $ThMn_{12}$-type crystal structure [2], space group I4/mmm, in which there are three nonequivalent crystal positions (8i, 8f and 8j) for Mn and one (2a) for Th.

In our program of studying rare earth iron-rich intermetallics relevant to permanent magnet applications, we focus our interest on the $RFe_{10}Cr_2$ series (R=Y, Nd, Gd, Tb, Dy, Ho, Er and Tm). In these compounds the 8i, 8f and 8j positions are occupied by Fe and M atoms while the 2a position are occupied by R atoms exclusively. Some results of our magnetic investigations of this series have been published elsewhere [14–18].

The ^{57}Fe Mössbauer effect technique was applied in studies of the $RFe_{10}M_2$ compounds quite extensively [19–23], mainly to determine the mode of site occupancy by M atoms and to extract the values of crystal field parameters, crucial for spin reorientation studies. It was established that for M=V, Ti and Mo there is a tendency to preferential site occupancy [20].

The purpose of this paper is to give some description of the magnetic properties of the $RFe_{10}Cr_2$ compounds (R=Y, Nd, Gd, Tb, Dy, Ho, Er and Tm) as observed with magnetic susceptibility and Mössbauer methods.

2. Experimental

Samples of nominal composition were prepared by induction melting of stoichiometric amounts of the constituent elements (99.9 wt % purity or better) in a water-cooled boat under an atmosphere of argon. The ingots were inverted several times to ensure homogeneity. The samples were then wrapped in a Ta foil, sealed in a quartz tube filled with argon and annealed for two weeks at 900°C and then rapidly cooled to room temperature. X-ray diffraction analysis was performed on powdered samples using CuKα radiation.

*Corresponding author.

0925-8388/98/$19.00
PII S0925-8388(97)00434-9

Magnetic measurements were performed, using the Weiss–Forrer method, in a temperature range from 78 to 900 K and in fields up to 2.6 T. The saturation magnetic moments were obtained from Honda plots while the Curie temperatures were determined from M^2 versus T curves (M is the magnetization and T the temperature). The anisotropy fields were measured on powders, sieved to 40 μm, aligned magnetically in wax.

The spin reorientation temperature was determined from measurements of the temperature dependence of the initial susceptibility using an ac bridge of mutual inductance of the Hartshorn type. The intensity of the alternating field used was 20 A m^{-1} and the frequency was 15 kHz.

The ^{57}Fe Mössbauer absorption spectra were recorded at room and liquid nitrogen temperatures using a ^{57}Co/Cr source, kept at room temperature, and a constant acceleration Mössbauer spectrometer. A high purity metallic iron foil was used for calibration of the velocity scale. Isomer shifts were established with respect to the centre of gravity of the iron Mössbauer spectrum. The least squares computer program was used to derive from Mössbauer absorption spectra the values of the hyperfine interaction parameters.

3. Results and discussion

The X-ray diffraction patterns of our compounds show only characteristic lines of the tetragonal $ThMn_{12}$ structure. The measured lattice parameters a and c, as well as unit cell volume V are plotted in Fig. 1 and listed in Table 1. All these parameters increase linearly with the radius of R^{3+} ion (c 1.5 times faster than a) except those for yttrium and erbium.

Table 1
Lattice constants a, c and cell volume V for various $RFe_{10}Cr_2$ compounds.

R	a [nm]	c [nm]	V [nm^3]
Y	0.8462	0.4762	0.34094
Nd	0.8556	0.4814	0.35233
Gd	0.8507	0.4769	0.34516
Tb	0.8506	0.4757	0.34424
Dy	0.8492	0.4753	0.34276
Ho	0.8475	0.4725	0.33935
Er	0.8534	0.4761	0.34670
Tm	0.8477	0.4675	0.33594

Errors: a and c (10^{-4} nm); V (1.5×10^{-4} nm^3)

The saturation magnetic moments per formula unit of the $RFe_{10}Cr_2$ compounds measured at 78 K and 295 K are plotted in Fig. 2 and listed in Table 2. These data indicate that the magnetic moments of R atoms in the $RFe_{10}Cr_2$ series are coupled to those of Fe atoms in a way similar to that observed in the binary R-Fe intermetallics. For compounds with light rare-earths ($J=L-S$) the total rare-earth magnetic moment (gJ) is coupled parallel to the iron magnetic moment, while for the heavy rare-earths ($J=L+S$) it is coupled antiparallel.

The values of saturation magnetic moments in the $RFe_{10}Cr_2$ series are substantially smaller than those in the $R_2Fe_{14}B$ compounds [24]. This is due to the smaller amount of iron per formula unit in undiluted samples and, additionally, due to the substitution of iron by chromium

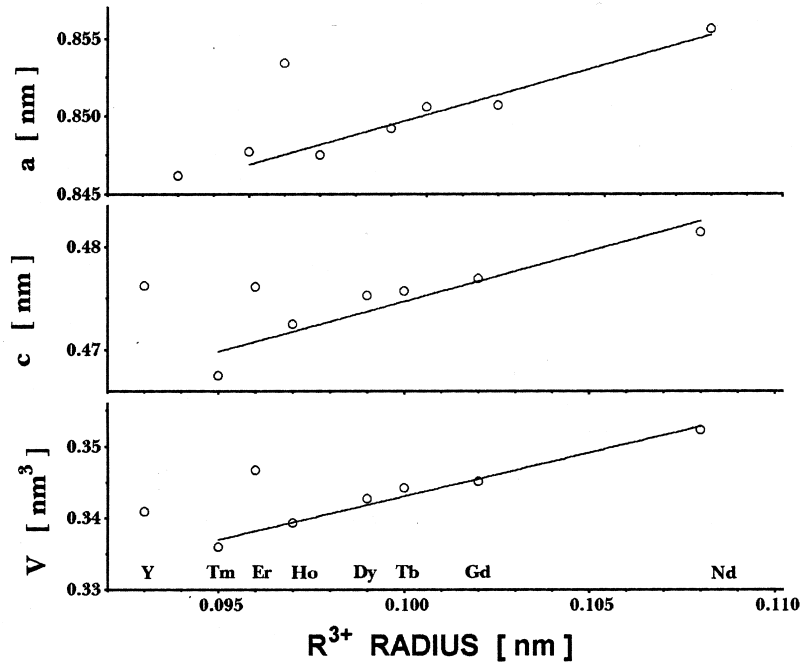

Fig. 1. Lattice constants and the unit cell volume in the $RFe_{10}Cr_2$ compounds as a function of the rare earth R^{3+} radius. The solid lines represent a linear regression when Y and Er were excluded.

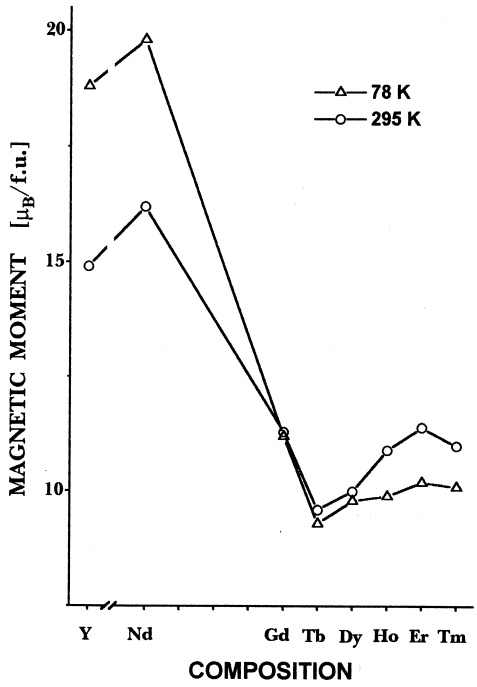

Fig. 2. Magnetic moments per formula unit of the $RFe_{10}Cr_2$ compounds measured at 78 K and 295 K. The solid line guides the eye.

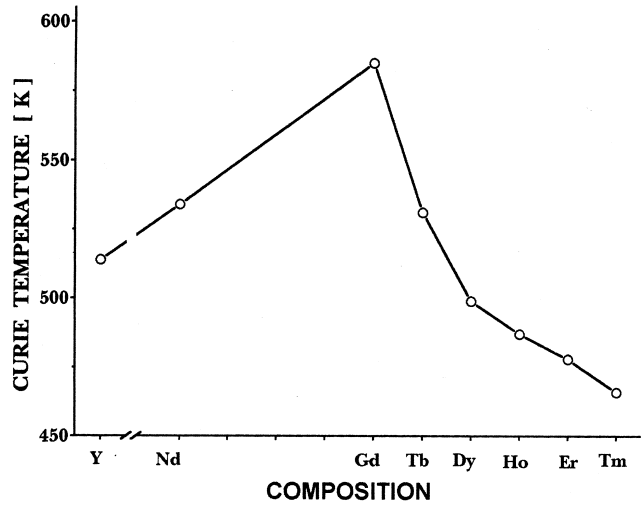

Fig. 3. Curie temperature for the $RFe_{10}Cr_2$ series. The solid line is a guide to the eye.

that shows a strong 8i site preference in the whole series of investigated compounds [this work]. Moreover, it seems that the replacement of Fe by Cr modifies the exchange interactions and thus leads to a decrease of the magnetization similarly as was observed in the $R_2Fe_{14-x}Cr_xB$ compounds [25].

The Curie temperatures of the $RFe_{10}Cr_2$ series are plotted in Fig. 3 and listed in Table 2. They obey the same trend as in the $R_2Fe_{14}B$ and other R-Fe compounds in which R=Gd takes the maximum value of the Curie temperature [24].

The values of the anisotropy field, obtained from intersection points of magnetization curves along easy and hard directions, are listed in Table 2. A substantial magnetic anisotropy field is found in the $YFe_{10}Cr_2$ compound although yttrium has no magnetic moment. This shows that also in the $RFe_{10}Cr_2$ series the Fe sublattice gives a considerable contribution to the magnetocrystalline anisotropy just like in the $Y_2Fe_{14}B$ compound [24].

Table 2
Magnetic properties of the $RFe_{10}Cr_2$ compounds: T_C Curie temperature, μ_s saturation magnetic moments per formula unit, H_A magnetic anisotropy field.

R	T_C [K]	μ_s [μ_B/f.u.]		H_A [T]
		78 K	295 K	
Y	514	18.8	14.9	2.6
Nd	534	19.8	16.2	4.6
Gd	585	11.2	11.3	2.7
Tb	531	9.3	9.6	[a]
Dy	499	9.8	10.0	4.9
Ho	487	9.9	10.9	4.0
Er	478	10.2	11.4	2.7
Tm	466	10.1	11.0	2.8

Errors: T_c (2 K); μ_s (0.1 μ_B); H_A (0.1 T)
[a] It seems that $TbFe_{10}Cr_2$ has an easy plane anisotropy.

In the $RFe_{10}Cr_2$ compounds the magnetic anisotropy of the rare earth sublattice prevails over that of the iron sublattices at low temperatures. Moreover, it decreases rapidly when the temperature increases and its sign depends on the rare earth element. On the other hand, the magnetic anisotropy of the iron sublattices is less sensitive to temperature and has a positive sign in the whole temperature range. When the rare earth and iron contributions to the magnetocrystalline anisotropy have opposite signs, a competition between them appears. It is manifested by a spin reorientation when the temperature changes. This phenomenon can be evidenced in the form of a distinct peak in the temperature dependence of the initial susceptibility curve as shown in Fig. 4 for the $DyFe_{10}Cr_2$ and $TbFe_{10}Cr_2$ compounds. The spin reorientation temperatures determined from the peak position for three selected samples of our series are as follows 298 K (for $TbFe_{10}Cr_2$), 190 K (for $DyFe_{10}Cr_2$) and 25 K (for $ErFe_{10}Cr_2$).

The crystal field and the corresponding rare earth sublattice anisotropy seem to be much weaker in the $R_2Fe_{12-x}T_x$ compounds than in the $R_2Fe_{14}B$ alloys. In the former compounds the absolute value of the second order crystal field parameter is about -130 K/a_0^2 and in the latter about 680 K/a_0^2 (both mean values) [4]. This implies that the hard magnetic properties of the $Nd_2Fe_{14}B$ type alloys are more favourable than those of the $RFe_{10}Cr_2$ compounds. This is confirmed by smaller values of the anisotropy fields in our compounds (Table 2).

Due to its high energy resolution, Mössbauer spectroscopy can provide a variety of useful information, basically of a local character, concerning the magnetic

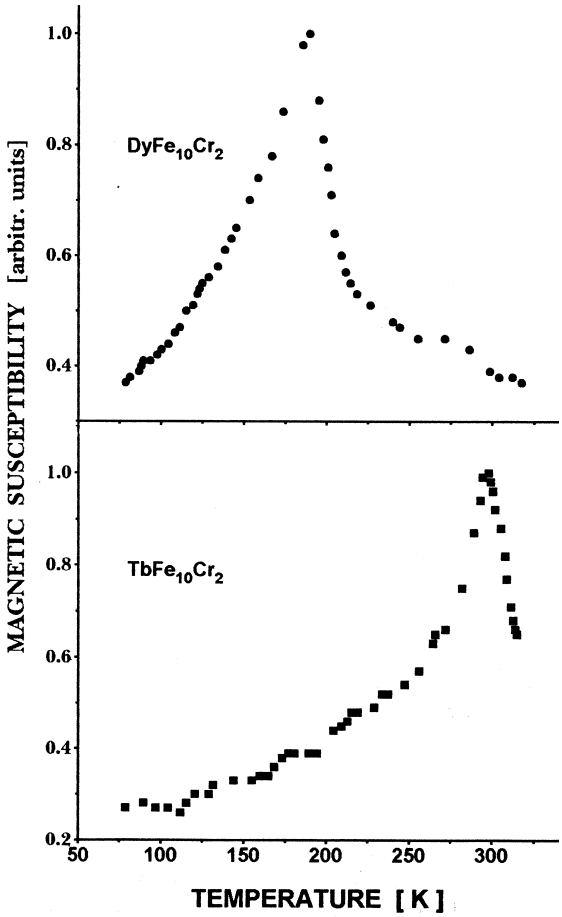

Fig. 4. Temperature dependence of the initial susceptibility of $DyFe_{10}Cr_2$ and $TbFe_{10}Cr_2$.

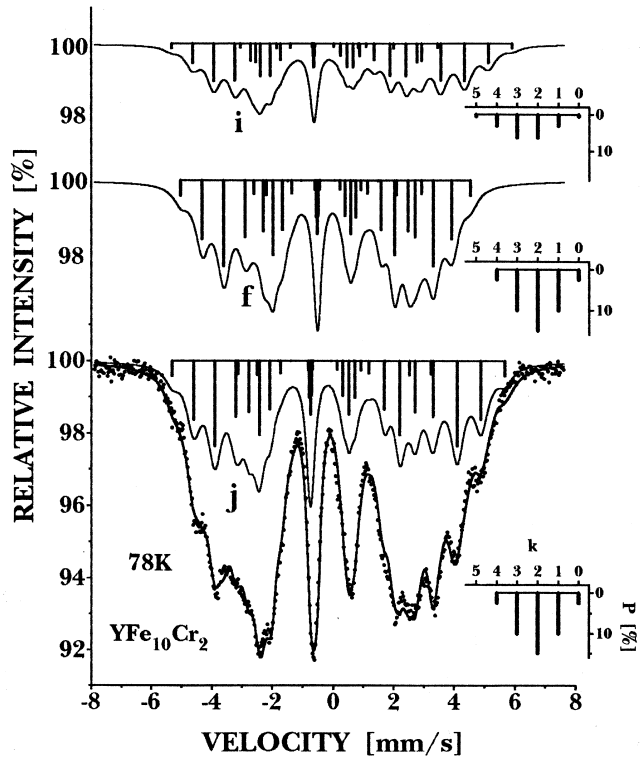

Fig. 5. ^{57}Fe Mössbauer spectrum of $YFe_{10}Cr_2$ at 78 K illustrating different contributions of sublattices to the overall spectrum. Insets show probability P that Fe is in a given sublattice and has k Cr nearest neighbours. The solid curves represent the computer fits.

structure of the materials studied. We applied this method to study the $RFe_{10}Cr_2$ compounds (R=Y, Gd, Tb, Dy, Ho, Er, Tm) with the main aim to determine average values of the hyperfine magnetic fields for the 8i, 8f and 8j sublattices and to search for the preferential site occupancy of Cr throughout the whole R-series. The selected ^{57}Fe Mössbauer spectra recorded for the $RFe_{10}Cr_2$ system at room and liquid nitrogen temperatures are shown in Fig. 5 and Fig. 6. Substitution of Cr for Fe in the $RFe_{10}Cr_2$ compounds creates various nearest neighbour atomic configurations of the nonequivalent 8i, 8f and 8j crystal sites. Due to this the Mössbauer absorption spectra are very complex. In order to derive the hyperfine parameters, the spectra were numerically resolved into Zeeman sextets. Each sextet is characterized by its hyperfine magnetic field, isomer shift and electric quadrupole interaction. Common to all sextets are three different linewidths and one line intensity ratio.

It proved impossible do decompose the spectra with only three Zeeman subspectra associated with the three nonequivalent crystal sites (Fig. 5). Therefore we used the statistical model based on Ref. [21], modified to suit our case. The main assumptions of this model are:

- Cr substituting Fe changes the nearest neighbourhood of iron and thus, instead of one Zeeman pattern associated with a given crystal site, one will observe a series of Zeeman patterns connected with the number of Cr atoms residing in the nearest neighbourhood of Fe,
- each Cr atom in the nearest neighbour shell of Fe decreases the hyperfine field by the same value,
- each Cr atom in the nearest neighbour shell of Fe changes the isomer shift (quadrupole splitting) by the same value.

We analyzed all possible configurations in the neighbourhood of Fe atoms in crystal position l (l=i, f, j), and calculated, using binomial distribution, the probabilities $P_l(k)$ that a given Fe atom, located in sublattice l, will have k Cr atoms in a shell of nearest neighbours,

$$P_l(k) = \sum_{n_i+n_j+n_f=k} \binom{m_i}{n_i} P_i^{n_i}(1-P_i)^{m_i-n_i} \times \binom{m_j}{n_j} P_j^{n_j}(1-P_j)^{m_j-n_j} \times \binom{m_f}{n_f} P_f^{n_f}(1-P_f)^{m_f-n_f},$$

where P_i, P_f and P_j are probabilities of finding Cr atoms in the respective sublattices ($P_i+P_f+P_j=0.5$), and where m and n are the total number of atoms and the number of Cr

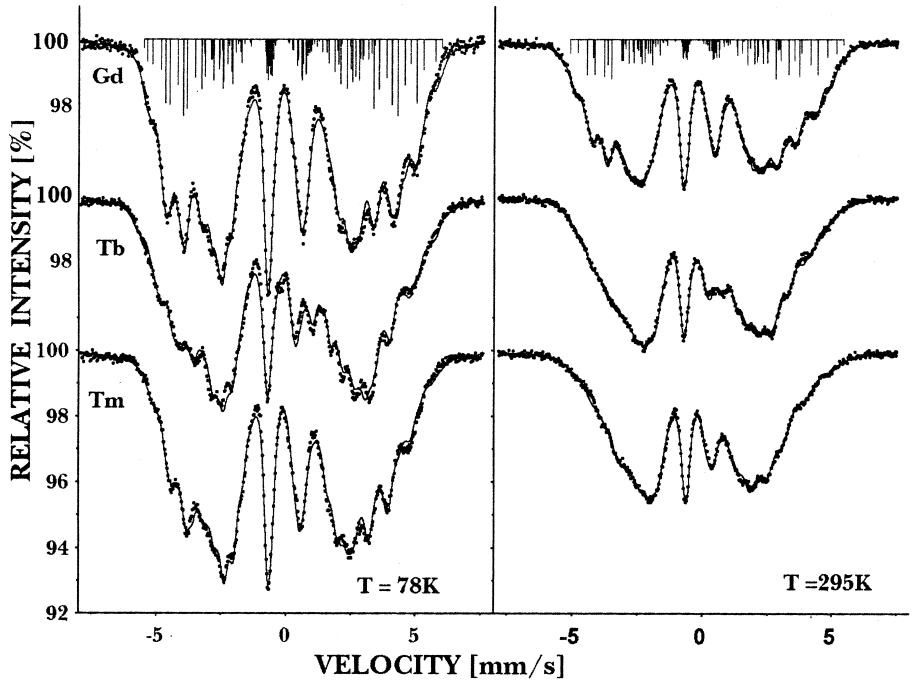

Fig. 6. Selected ^{57}Fe Mössbauer spectra recorded for the $RFe_{10}Cr_2$ compounds at 78 and 295 K. The solid curves represent the computer fits. In the terbium sample the spin reorientation takes place at 298 K but it is not completed yet at 295 K.

atoms in a nearest neighbourhood belonging to the respective sublattices.

In the fitting procedure the relative intensities of the different subspectra were set proportional to $P_1(k)$. The hyperfine field (H), the isomer shift (IS) and the quadrupole splitting (QS) were assumed to change linearly with the number of Cr neighbours of each 8i, 8f and 8j crystal site. The six the most intense subspectra were considered for each sublattice, resulting in 18 Zeeman sextets for a given Mössbauer spectrum. Fig. 5 shows, as an example, the ^{57}Fe Mössbauer spectrum of $YFe_{10}Cr_2$ illustrating how the 8i-, 8f-, and 8j-sublattices contribute to the overall spectrum. It is typical throughout the whole series that 8i-sublattice has the smallest contribution. The line bar diagrams show the line intensities that are proportional to the probabilities P (see inset) that Fe is in a given sublattice and has k nearest Cr neighbours. Several other selected Mössbauer spectra are shown in Fig. 6. The values of the hyperfine interaction parameters derived from the spectra for all investigated compounds, assigned to crystal lattices are shown in Fig. 7. It is seen that the rare earth ions have little influence on the hyperfine interaction parameters. The anomaly observed for Tb may be due to the spin reorientation effect (298 K) which is not completed yet at 295 K. Fig. 8 shows the probabilities P_i, P_f and P_j (obtained from fits) of finding Cr in the respective sublattices. It is clearly seen that Cr shows a definite preference for occupying the 8i sublattice in the whole series of investigated compounds. An explanation of such preference may be given in terms of a combination of size effects and enthalpy effects [12].

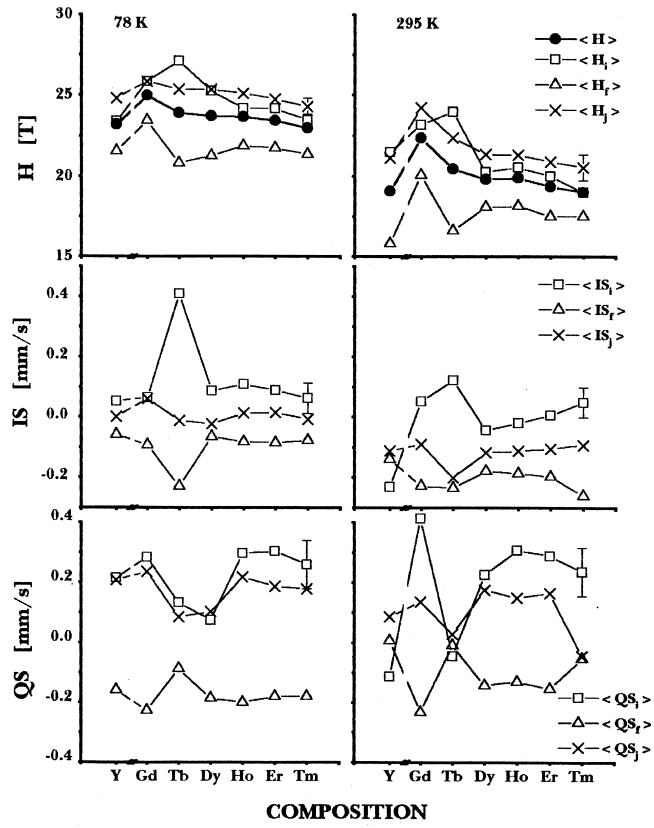

Fig. 7. Hyperfine interaction parameters derived from the ^{57}Fe Mössbauer spectra of the $RFe_{10}Cr_2$ compounds. The solid lines are guides to the eye. In the terbium sample a spin reorientation takes place at 298 K but it is not completed yet at 295 K.

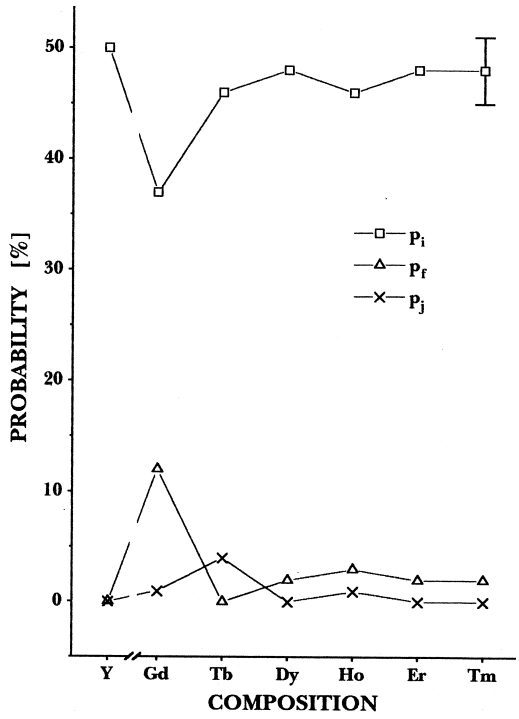

Fig. 8. Probabilities P_i, P_f and P_j of finding Cr in 8i, 8f, and 8j sublattices, respectively, derived from the ^{57}Fe Mössbauer spectra. The solid lines are guides to the eye.

The magnetic susceptibility and Mössbauer effect data can be used to determine the approximate values of the magnetic moments for the iron and rare earth ions. From the molecular magnetic moment of $YFe_{10}Cr_2$ (Table 2) it follows that the average iron magnetic moment is 1.88 μ_B at 78 K and 1.49 μ_B at 295 K. With these values and the average values of the ^{57}Fe hyperfine fields for $YFe_{10}Cr_2$ at the temperatures considered (Table 3) one can compute the conversion factors 12.34 μ_B/T (at 78 K) and 12.82 μ_B/T (at 295 K) between the hyperfine magnetic fields and magnetic moments. Unfortunately, the corresponding helium temperature data for our compounds are lacking. Therefore we have assumed, in the rough approximation, that these factors are valid for the whole series of the investigated $RFe_{10}Cr_2$ compounds and we have used them in our calculation of the average values of the iron magnetic moments in the 8i, 8f and 8j crystal sites and of the overall average values (Table 4). When a collinear ordering of the iron and rare earth sublattices is assumed, the values of molecular magnetic moments of our compounds listed in Table 2 and the average moment values of the iron ions at three crystal sites give us the approximate values of magnetic moments of rare earth ions (Table 4).

Table 4
Approximate values of the iron (μ_{Fe}) and rare earth (μ_R) magnetic moments derived from magnetic susceptibility and Mössbauer data.

R	T	μ_{Fe} [μ_B]			$\langle\mu_{Fe}\rangle$	μ_R [μ_B]
	[K]	i	f	j	[μ_B]	
Y	78	1.90	1.74	2.01	1.88	0
	295	1.68	1.23	1.65	1.49	0
Gd	78	2.09	1.90	2.09	2.03	−1.5
	295	1.81	1.57	1.89	1.73	−2.4
Tb	78	2.20	1.69	2.05	1.94	−10.1
	295	1.87	1.29	1.75	1.60	−6.4
Dy	78	2.04	1.65	1.97	1.85	−8.7
	295	1.58	1.41	1.66	1.54	−5.4
Ho	78	1.96	1.77	2.03	1.91	−9.2
	295	1.60	1.41	1.66	1.55	−4.6
Er	78	1.95	1.76	2.00	1.90	−8.8
	295	1.56	1.37	1.63	1.51	−3.7
Tm	78	1.90	1.73	1.97	1.86	−8.5
	295	1.56	1.37	1.63	1.51	−4.1

Errors: T (1 K); μ_{Fe} (<0.16 μ_B); $\langle\mu_{Fe}\rangle$ (<0.12 μ_B); μ_R (<1.3 μ_B)

Table 3
Average values of the ^{57}Fe hyperfine interaction parameters derived from Mössbauer spectra for the 8i, 8f and 8j sublattices of the $RFe_{10}Cr_2$ intermetallic compounds.

R	T [K]	IS [mm s^{-1}]			QS [mm s^{-1}]			H [T]			$\langle H\rangle$ [T]
		i	f	j	i	f	j	i	f	j	
Y	78	0.05	−0.06	0.00	0.21	−0.16	0.21	23.4	21.5	24.8	23.2
	295	−0.23	−0.14	−0.11	−0.11	0.01	0.08	21.5	15.8	21.1	19.1
Gd	78	0.06	−0.09	0.06	0.28	−0.23	0.23	25.8	23.4	25.8	25.0
	295	0.05	−0.23	−0.09	0.41	−0.23	0.14	23.2	20.1	24.2	22.2
Tb	78	0.41	−0.23	−0.01	0.13	−0.09	0.08	27.1	20.8	25.3	23.9
	295	0.12	−0.24	−0.20	−0.04	−0.01	0.03	24.0	16.6	22.4	20.5
Dy	78	0.09	−0.07	−0.02	0.07	−0.18	0 10	25.2	21.2	25.3	23.7
	295	−0.04	−0.18	−0.12	0.22	−0.14	0.17	20.2	18.1	21.3	19.8
Ho	78	0.11	−0.08	0.01	0.30	−0.20	0.22	24.2	21.8	25.1	23.6
	295	−0.02	−0.19	−0.11	0.30	−0.13	0.15	20.5	18.1	21.3	19.9
Er	78	0.09	−0.09	0.01	0.30	−0.18	0.18	24.1	21.7	24.7	23.4
	295	0.01	−0.20	−0.11	0.29	−0.15	0.16	20.0	17.5	20.9	19.4
Tm	78	0.06	−0.08	−0.01	0.26	−0.18	0.18	23.4	21.3	24.3	23.0
	295	0.05	−0.26	−0.11	0.23	−0.05	0.16	20.0	17.5	20.9	19.4

The parameters listed have the following meaning: IS, isomer shift with respect to metallic iron at room temperature; QS, quadrupole shift of the spectra lines $[(V6-V5)-(V2-V1)]/2$; H, hyperfine magnetic field; $\langle H\rangle$, average value of the hyperfine magnetic field at three crystal sites. Errors: T (1 K); IS (0.05 mms^{-1}); QS (0.08 mms^{-1}): H (0.9 T); $\langle H\rangle$ (0.4 T)

All of them, excepting Gd are similar to those reported for the $R_2Fe_{14}B$ compounds [26].

In conclusion, magnetic susceptibility measurements and Mössbauer spectroscopy enabled us to determine the bulk properties (the Curie temperature, the saturation magnetization, the spin reorientation) and microscopic properties (the ^{57}Fe hyperfine interaction parameters, the average magnetic moments of iron and the moments of some rare earth atoms) of the $RFe_{10}Cr_2$ compounds. Both methods proved to be complementary in describing the magnetism in this class of materials.

References

[1] D.B. de Mooij, K.H.J. Buschow, J. Less-Common Met. 136 (1988) 207.
[2] D.B. de Mooij, K.H.J. Buschow, Philips J. Res. 42 (1987) 246.
[3] F.R. de Boer, Huang Ying-Kai, D.B. de Mooij, K.H.J. Buschow, J. Less-Common Met. 135 (1987) 199.
[4] K.H.J. Buschow, D.B. de Mooij, M. Brouha, H.H.A. Smith, R.C. Thiel, IEEE Trans. Magn. MAG 24 (1988) 1611.
[5] P.C.M. Gubbens, A.M. van der Kraan, K.H.J. Buschow, Hyperfine Interactions 40 (1988) 389.
[6] R.B. Helmholdt, J.J.M. Vleggaar, K.H. J Buschow, J. Less-Common Met. 144 (1988) 209.
[7] R. Verhoef, F.R. de Boer, Zhang Zhi-dong, K.H.J. Buschow, J. Magn. Magn. Mat. 75 (1988) 319.
[8] K.H.J. Buschow, J. Less-Common Met. 144 (1988) 65.
[9] Bo-Ping Hu, Hong-Shuo Li, J.P. Gavigan, J.M.D. Coey, J. Phys. Condens. Mat. 1 (1989) 755.
[10] W.G. Haije, J. Spijkerman, F.R. de Boer, K. Bakker, K.H.J. Bushow, J. Less-Common Met. 162 (1990) 285.
[11] X.P. Zhong, F.R. de Boer, D.B. de Mooij, K.H.J. Buschow, J. Less-Common Met. 163 (1990) 123.
[12] K.H.J. Buschow, J. Magn. Magn. Mat. 100 (1991) 79.
[13] H.S. Li, J.M.D. Coey, in: Handbook of Magnetic Materials, K.H.J. Buschow, (Ed.), vol. 6, North Holland Publ., Amsterdam, 1994, p. 1.
[14] P. Stefański, A. Kowalczyk, A. Wrzeciono, J. Magn. Magn. Mat. 81 (1989) 155.
[15] P. Stefański, A. Kowalczyk, A. Wrzeciono, J. Magn. Magn. Mat. 83 (1990) 145.
[16] P. Stefański, A. Kowalczyk, A. Wrzeciono, J. Magn. Magn. Mat. 101 (1991) 97.
[17] P. Stefański, Solid State Commun. 74 (1990) 731.
[18] P. Stefański, A. Kowalczyk, Solid State Commun. 77 (1991) 397.
[19] T. Sinnemann, M. Rosenberg, K.H.J. Buschow, J. Less-Common Met. 146 (1989) 223.
[20] T. Sinnemann, K. Erdmann, M. Rosenberg, K.H.J. Buschow, Hyperfine Interactions 50 (1989) 675.
[21] C. Christides, A. Kostikas, A. Simopoulos, D. Niarchos, G. Zouganelis, J. Magn. Magn. Mat. 86 (1990) 367.
[22] T. Sinnemann, M.U. Wisniewski, M. Rosenberg, K.H.J. Buschow, J. Magn. Magn. Mat. 83 (1990) 259.
[23] C.J.M. Denissen, R. Coehoorn, K.H.J. Buschow, J. Magn. Magn. Mat. 87 (1990) 51.
[24] S. Sinnema, R.J. Radwański, J.J.M. Franse, D.B. de Mooij, K.H.J. Buschow, J. Magn. Magn. Mat. 44 (1984) 333.
[25] A. Kowalczyk, A. Wrzeciono, Phys. Stat. Sol., (a) 109 (1988) 884.
[26] J.F. Herbst, Rev. Modern Phys. 63 (1991) 819.